

Superconductor Joule Losses in the Zero-Field-Cooled Maglev Vehicle

J. Fernandes, I. Montes, R. Sousa, C. Cardeira, and P. J. Costa Branco

Abstract—This paper estimates for the first time the Joule losses in the YBCO superconductors in the zero-field-cooled (ZFC) Maglev vehicle. Imposing a pendulum-like movement to the vehicle and since the aerodynamic losses were taken into account in the experiments, obtained results show that the Joule losses occurred in the superconductors during the vehicle's movement. Four movement tests were completed, which allow measuring the average losses in superconductors that were responsible by vehicle's damping. A finite-element model of the vehicle showed how and why YBCO Joule losses are function of the vehicle speed. It quantifies the losses and indicates that, in the ZFC-Maglev, these are clearly reduced since the significant losses are located only in a very small layer at the superconductors' surface.

Index Terms—FEM modeling, HTS, Maglev, magnetic levitation, power losses, YBCO, ZFC-Maglev.

I. INTRODUCTION

TRADITIONAL Field-Cooled (FC) Maglev vehicles have two drawbacks: effect of field cooling heights producing smaller levitation density forces and, as designated by Costa Branco *et al.* [1], important Joule losses in the bulk superconductors will be present due to superconductors field cooling process. To minimize these problems, a new Maglev design was proposed in [2] that uses only zero-field cooled (ZFC) superconductors in a track having only NdFeB permanent magnets. However, it lacked quantifying the Joule losses in the superconductors. Since the levitation system is composed of passive elements, the most significant operational cost will be the cooling system for the superconductors, in order for them to be in their superconductive state at temperatures below the 90 K. This makes the required quantity of liquid nitrogen to cool the superconductor blocks the main operational cost.

The paper begins experimentally quantifying the superconductors Joule losses in the ZFC Maglev using a pendulum like rail as shown in Fig. 1. Aerodynamic losses during the vehicle's movement were taken into account. Hence, several movement tests were completed, which allowed measuring the average Joule losses in superconductors that were responsible by ZFC



Fig. 1. Pendulum rail for the Joule losses experiment with the ZFC-Maglev.

vehicle's damping. For a better understanding of achieved results, the development of a finite element model (FEM) for the YBCO including its hysteresis characteristic was required. With this model and after its experimental validation, power losses in the superconductors were estimated as function of Maglev speed. This also allowed the characterization of the possible liquid nitrogen consumption in the ZFC Maglev.

II. ZFC-MAGLEV VEHICLE CONFIGURATION

The basic structure of the ZFC-Maglev is shown in Fig. 2(a). It consists of four YBCOs overlapped over twelve NdFeB magnets. The two superconductors' lines are separated by an air-gap. The lateral magnets have their polarization according to the positive direction of the z axis, while the central row magnets have opposite polarization.

A ZFC-Maglev alternative has been proposed by Dente and Branco [2] consists in a new track topology shown in Fig. 2(a). As shown in Fig. 2(b), the track takes advantage of ZFC Meissner effect to levitate and lock the superconductors in place, by making the field lines close around the superconductors, thus producing a resultant guidance force in the vehicle. In Fig. 2(b) one verifies that this is achieved by placing two columns of superconductors, thus allowing the magnetic field to close through the air-gap between them.

In order to get the guidance forces, each superconductor must have a width value less than the distance between the magnets' central axis. Therefore, the superconductors become confined among the three regions (1)–(3) which are marked in Fig. 2(b). In region (1), the vertical component of the magnetic field, which value is nearly the maximum magnetic field value of the magnet, is responsible by the force exerted

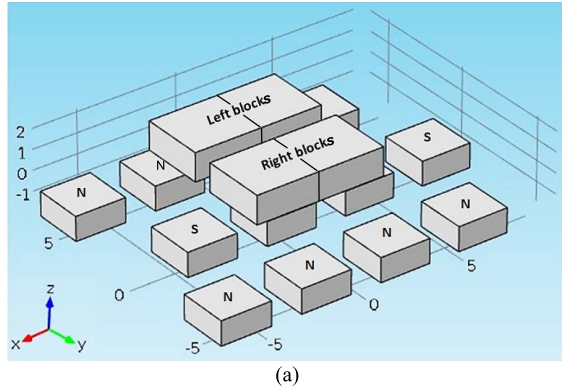
Manuscript received September 6, 2015; accepted January 20, 2016. Date of publication February 11, 2016; date of current version May 4, 2016. This work was supported by FCT, through IDMEC, under LAETA, project UID/EMS/50022/2013. (Corresponding author: P. J. Costa Branco.)

J. Fernandes, I. Montes, and R. Sousa are with the Department of Mechanical Engineering, Instituto Superior Técnico, Universidade de Lisboa, 1049-001 Lisbon, Portugal.

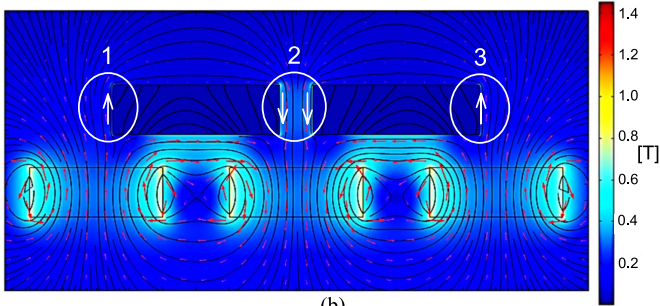
C. Cardeira and P. J. Costa Branco are with LAETA, IDMEC, Instituto Superior Técnico, Universidade de Lisboa, 1049-001 Lisbon, Portugal (e-mail: carlos.cardeira@tecnico.ulisboa.pt; pbranco@tecnico.ulisboa.pt).

Color versions of one or more of the figures in this paper are available online at <http://ieeexplore.ieee.org>.

Digital Object Identifier 10.1109/TASC.2016.2528991



(a)



(b)

Fig. 2. (a) ZFC track and superconductors' placement. (b) Proposed track topology: The superconductors are locked in place by the permanent magnets' field.

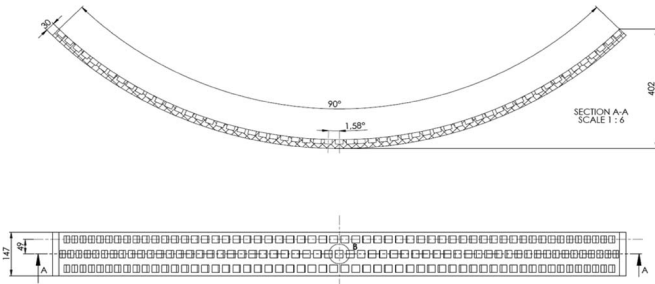
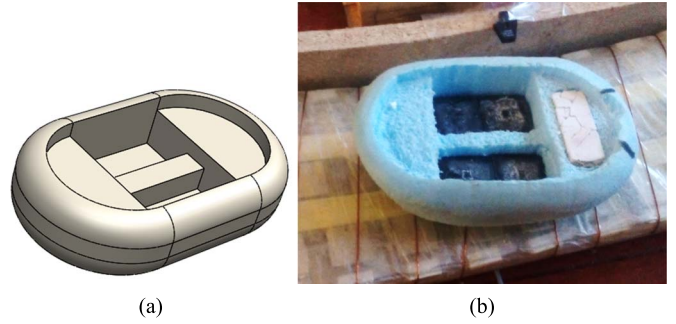


Fig. 3. Design schematic of the pendulum rail and photo of the structure built in our laboratory.

to the right on the superconductors' first column. Similarly in region (3), an electromagnetic force to the left is generated in the superconductors' second column in right lateral surface. The design of the ZFC-based Maglev also includes region (2). This is located between the two superconductor tracks and reinforces the lateral stability of the vehicle using the same effect as occurred in regions (1) and (3), but now with the electromagnetic forces actuating at the same time on each superconductor's lateral surfaces.

When using the proposed ZFC-maglev approach, pinning is totally irrelevant. However, critical current density continues to be important since it will also affect how large will be force densities at each superconductor surface, thus levitation and guidance ones.

The pendulum track design used by the ZFC-Maglev is shown in Fig. 3. This type of track consists only of permanent magnets and aluminum as a fitting to keep the magnets in place. Although in Fig. 3 bottom draw could suggest a non-equidistant arrangement of the Permanent Magnets (PMs) at both rail ends, this is not the case. All PMs at each column are equidistant.



(a)

(b)

Fig. 4. (a) Recipient design to contain the set of four YBCO superconductors. (b) Photo of the vehicle built with the superconductors already in place.



Fig. 5. Photo of the rail with the optical sensors distributed along the track and the Arduino microcontroller circuit to process all sensors data.

A. Pendulum Rail Structure and the Vehicle

Fig. 3 shows a schematic of rail, which has an arc-shaped to allow the vehicle to execute a pendulum like movement. Except PMs, the embedding and rail construction materials were non-magnetic to avoid any interference with them.

Fig. 4(a) shows the vehicle configuration designed to store the superconductors in a way they would maintain the correct distance between themselves (1 cm). The vehicle also has an extra space to store a small amount of liquid nitrogen to maintain the superconductors under its critical temperature during the tests. The vehicle was built with polyurethane [blue material in Fig. 4(b)] since it is easy to use, impermeable and has a very good thermal insulation. Two sets of two YBCOs were placed inside the vehicle side by side as shown in Fig. 4(b).

B. Position Sensors

The pendulum rail was equipped with a set of optical sensors (HOA1405-002) that acquire data related to the movement of the vehicle, as shown in Fig. 5. These sensors were placed along the rail in an equidistant way, which allowed the measurement of the time that the vehicle takes between them. With this time and with the length of the vehicle, it was possible to estimate its speed at each location. Data acquired by sensors are sent to an Arduino Uno microcontroller, which sends the values through a serial port monitor, ready to be processed.

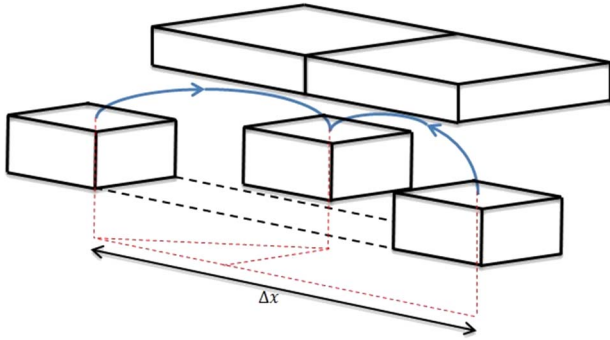


Fig. 6. Symbolic illustration of the distance Δx , for which a time period is defined for the magnetic field acting on the superconductors.

III. JOULE LOSSES IN THE ZFC-MAGLEV

To understand how Joule losses occur in the superconductors when the vehicle moves along its PM track, consider just a half cross section of the levitation system as shown in Fig. 6. See the representation of the magnetic field distribution below the superconductors. The figure indicates the distance Δx for which a time period is defined according to vehicle speed v . From this value, the frequency f for the magnetic field between the centers of two consecutive superconductors and lateral permanent magnets was calculated using Eqs. (1) and (2)

$$v = \frac{\Delta x}{\Delta t} \rightarrow \Delta t = \frac{\Delta x}{v} \quad (1)$$

$$f = \frac{1}{\Delta t} \rightarrow f = \frac{v}{\Delta x}. \quad (2)$$

IV. QUANTIFICATION OF YBCOs' JOULE LOSSES

In the experiment, the vehicle speed measured was assumed that in the lowest point of the rail the variation of potential energy per cycle is zero. Hence, the variation of kinetic energy between two consecutive speed measurements will be equal to the total energy losses in the system as expressed by (3)

$$\frac{1}{2}m(v_i^2 - v_f^2) = E_{aero} + E_{joule}. \quad (3)$$

Since the speed is obtained using optical sensors, it was possible to obtain the aerodynamic losses. It consisted in obtaining the speed variation of the vehicle without interacting with the permanent magnets. The vehicle was suspended in a circular bar, as shown in Fig. 7(a) and (b), being the distance to the axis equal to the curvature radius of the pendulum rail.

With that approach, data related with the speed of the vehicle per cycle was acquired. Equation (4) was then used to compute the accumulated losses for each cycle. In (4), v_0 is the first speed measured, v_f is the speed measured in the n th cycle, and $E_{aero}(n)$ is the accumulated aerodynamic losses until the n th cycle. Fig. 8 plots the accumulated aerodynamic losses by green dots

$$\frac{1}{2}m(v_0^2 - v_f^2) = E_{aero}(n). \quad (4)$$

If the speed is known in two consecutive time instants, the energy losses only due to the Joule effect in the superconductors can be calculated using (5). These are plotted in Fig. 8 by red dots

$$\frac{1}{2}m(v_0^2 - v_f^2) - E_{aero}(n) = E_{joule}. \quad (5)$$

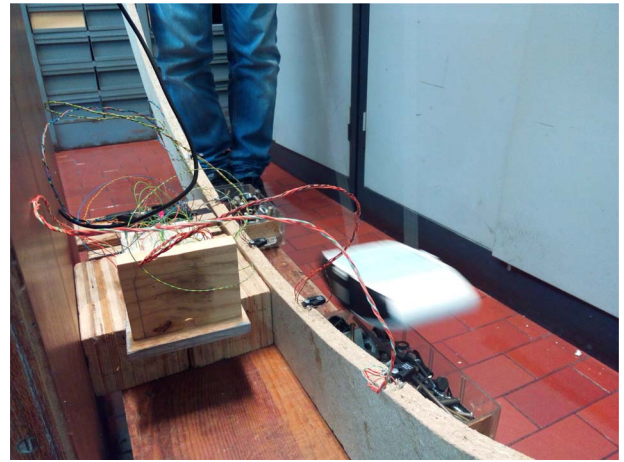
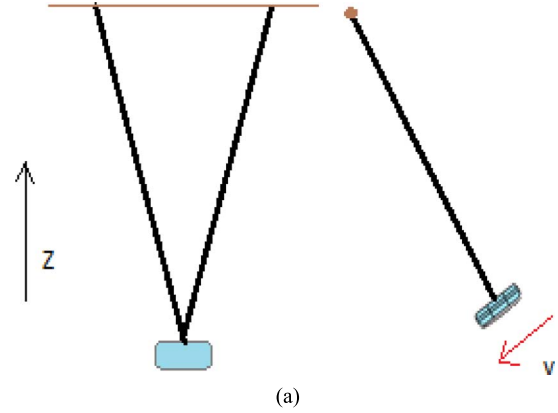


Fig. 7. Scheme of the experimental setup to obtain the aerodynamic losses.

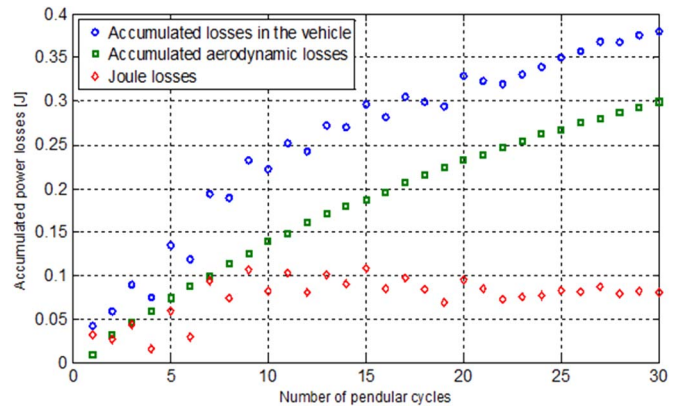


Fig. 8. Accumulated total losses (blue points), aerodynamic losses (green points), and accumulated Joule losses in the superconductors (red points).

V. YBCOs MODEL AND ITS EXPERIMENTAL VALIDATION

For a better understanding of the results achieved in Fig. 8, a FEM electromagnetic model for simulation of bulk YBCO superconductors and their hysteretic magnetization was developed. The properties of the YBCO under the influence of slow time-varying magnetic fields were studied. Its Joule losses are analyzed with respect to the characteristics of the external applied magnetic field (B amplitude and frequency).

The approximation of a type II superconductor in ZFC condition to a magnet leads to the circulation of electric currents

in its volume, which have larger values in the surfaces, so that the external magnetic field is repelled. From these currents it is possible to determine the electrical and magnetic field distribution in the superconductors volume and so the existent internal Joule losses.

A. Electromagnetic Equations

The levitation system is composed by two elements: permanent magnets and type II superconductors. Hence, the model considered three distinct regions: the air, the superconductors and the permanent magnets. It is assumed that the polyurethane and air magnetic features are the same. In the air and in the superconductor regions, the density current (\mathbf{J}) and the magnetic field (\mathbf{H}) are established by Eqs. (6) and (7). The only difference between the two regions, air and superconductor, is the constitutive relation (8) or (9) by which the electrical field (\mathbf{E}) is defined. The magnets region is considered only as a field source one, and it was modeled so that it had the remnant magnetic flux density of the magnets.

The computation of density currents ($\mathbf{J} = [J_x, J_y, J_z]$) and the magnetic field components ($\mathbf{H} = [H_x, H_y, H_z]$) are common to all regions, being taken directly from Maxwell's equations for a quasi-stationary regime

$$\mathbf{J} = \nabla \times \mathbf{H} \quad (6)$$

$$\nabla \times \mathbf{E} = -\frac{\partial \mathbf{B}}{\partial t}. \quad (7)$$

The air is considered a linear region where its constitutive relation is given by eq. (8), where ρ is its electrical resistivity

$$\mathbf{E}_{\text{air}} = \rho \mathbf{J}. \quad (8)$$

It has been used a macroscopic modeling approach of type II superconductors. The key departure comes in the form of their non-linear $E-J$ relationship that takes the form of relation (9), which is function of the superconductor parameters: E_0 , $J_c(B)$, n , and B_0 . The $J_c(B)$ critical density current is given by (10), showing its dependency of the magnetic flux density

$$\mathbf{E}_{\text{SC}} = E_0 \left(\frac{J_{\text{SC}}}{J_c(B)} \right)^n \quad (9)$$

$$J_c(B) = \frac{J_{c0} B_0}{B_0 + \|\mathbf{B}\|}, \|\mathbf{B}\| = \mu_0 \mu_r \sqrt{H_x^2 + H_y^2 + H_z^2}. \quad (10)$$

Parameter n represents the possible states of conductivity by the superconductor [3]. When it is 1, the superconductor is in its resistive state. When it goes to infinite, the superconductor is in the ideal superconductive state, that is, $E_{\text{SC}} = 0$ in all superconductor volume. The E_0 parameter has the value of the critical electrical field.

The computation of $J_c(B)$, J_{c0} , and B_0 values depend on the type of superconductor used. These parameters essentially regulate the density current in function of the norm of the magnetic flux density applied to the superconductor. Table I lists the values of the YBCO used in the FEM model. To calculate the electromagnetic forces in the superconductor's surface, the Maxwell Stress Tensor was used.

TABLE I
YBCO PARAMETERS USED IN THE FEM MODEL

B_0	0,1 T
J_{c0}	2×10^7 A/m ²
E_0	1×10^{-4} V/m
n	21

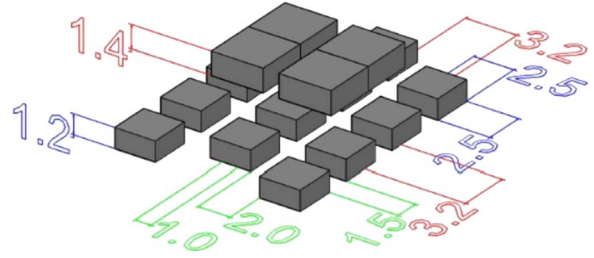


Fig. 9. ZFC track and superconductor placement. A mesh of 0.5 cm was used.

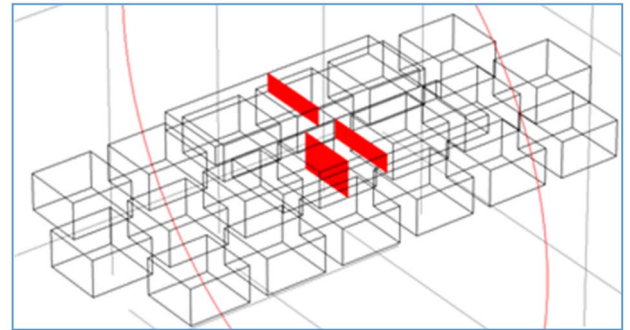
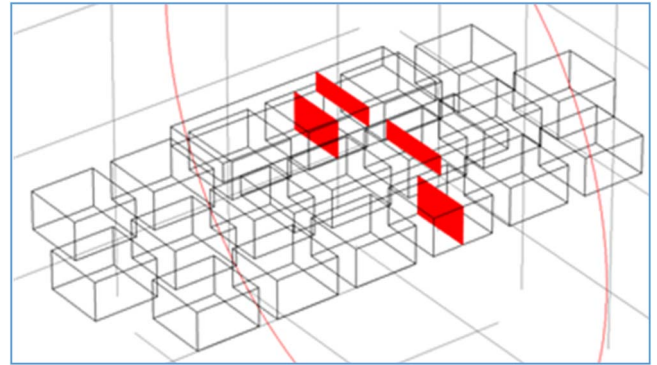


Fig. 10. Two cuts made in the yz plane along the x -direction.

B. Model Verification and Validation

The 3D FEM results from the ZFC-Maglev model were compared with the experimental results obtained from the prototype vehicle (Fig. 4). Its dimensions are indicated in Fig. 9. There is an air gap of 1 cm between the superconductors, and the magnets have a spacing of 1.5 cm over x direction and of 2 cm over the y direction.

By making a cut along the yz plane in Fig. 9, in such a way that it intersects the magnets and the superconductors, the distribution of magnetic field B in 3D space can be observed. However, notice that, due to the offset between the lateral magnets and the central ones, two cuts had to be made in two different places along the x direction, as shown in Fig. 10.

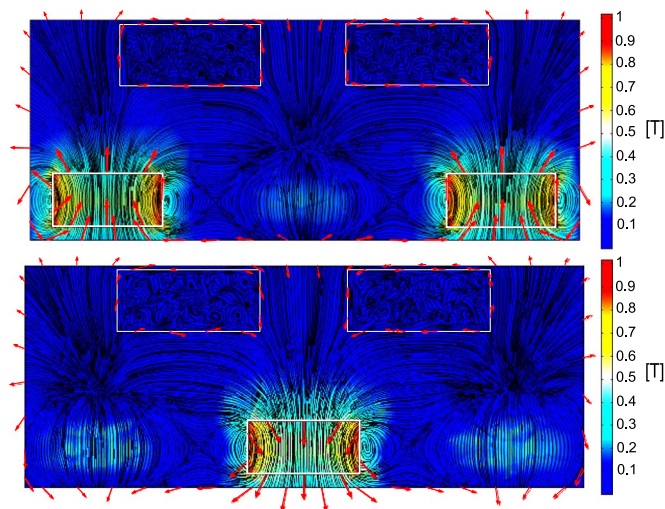


Fig. 11. Cuts made in the yz plane along the x -direction.

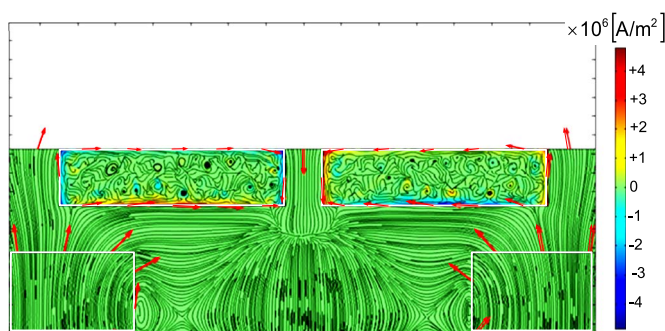


Fig. 12. Visualization of the electric current density and the magnetic flux distribution lines within the superconductors.

In Fig. 11, the upper graph shows the plane that cuts the two lateral magnets. These have the same polarity and are responsible for the tangential magnetic field below the superconductors and ends in the magnet located in the middle seen in the lower graph of Fig. 11. In both graphs, streamlines were used to compose a map of the magnetic field distribution in the ZFC-Maglev system. Both graphs also show that the magnetic flux closes around the borders of the superconductor blocks, as indicated by red arrows.

Fig. 12 shows that within the superconductors there are flux lines closed in a spiracle shape, which points to the transverse components of the internal electric currents. These results clearly show that in the ZFC condition the superconductors will have stronger currents near their borders, having very small current values within its core. In conclusion, the model is pointing out that the YBCO Joule losses in the ZFC-Maglev will be located in a very small volume located around the superconductor borders, which indicates *a priori* very small Joule losses.

Using the model, levitation forces were also computed for different air gaps between the vehicle and the permanent magnet track. This was essential to validate the model in a simple way, where the levitation forces were also measured using the experimental setup shown in Fig. 13.

To obtain the levitation forces, a piezoelectric force sensor Scaime K12+LMV shown in Fig. 13(a) was used. Fig. 13(b)

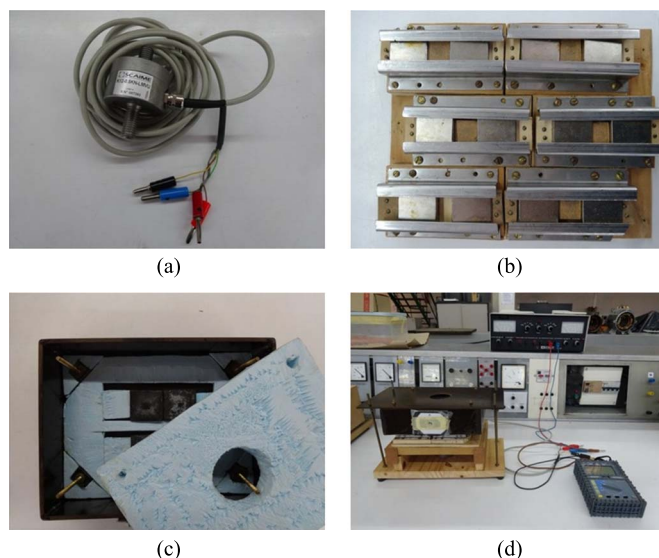


Fig. 13. Experimental setup. (a) Piezoelectric force sensor. (b) Track module. (c) Disposition of the superconductors inside the foam box following the same geometry used in the simulation. (d) Total assembly for the experiment.

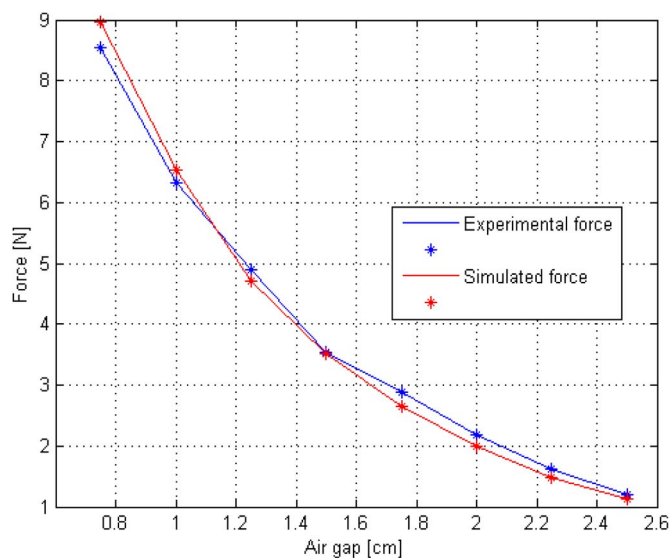


Fig. 14. Mode levitation force with the measured one for the ZFC-Maglev.

shows a photo of a track module built for this experiment. Fig. 14(c) shows the four YBCOs in columns of two within a foam box having equal dimensions as those used in the FEM model. At last, the complete setup used is presented in Fig. 13(d).

Fig. 14 shows the levitation forces previewed by the model and those ones measured in the lab in a descend direction. Results show only descend curve, which was enough to validate the model developed. The results show a consistent small error between those experimental and model values on an average value of 11%. This error comes from the numerical precision associated with the mesh used in the FEM simulation. This could be removed using a finer mesh. However, the computational effort was too much for current hardware. Therefore, since the order of the error values was almost independent of the air gap value, the FEM model was considered validated with good precision.

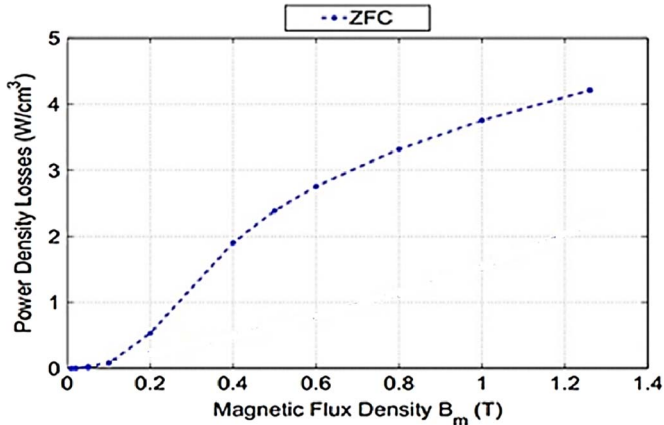


Fig. 15. ZFC-Maglev power loss density in function of the magnitude of the applied magnetic field over the superconductor for 5-Hz magnetic field frequency.

VI. JOULE LOSSES AT ZFC-MAGLEV AND ASSOCIATED OPERATIONAL COSTS

Joule losses in the superconductors of the ZFC Maglev are estimated in this section using the previous FEM model. As the levitation system is composed of passive elements, the only significant operational cost for the vehicle will be the cooling system for the superconductors in order for them to be in their superconductive state at temperatures below the 90 K. This makes the required quantity of liquid nitrogen to cool the superconductors the main operational cost.

To obtain a quantitative value of the liquid nitrogen needed, the FEM model was used now to evaluate the superconductor power losses as function of the amplitude and frequency of an external applied magnetic field. Notice that different frequency values means different vehicle speeds as already explained in Section IV.

Using the results from Figs. 11 and 12, it was possible to calculate the average value of the magnetic field that crosses the inferior surface of the superconductor blocks (B_z), which had about 1 mT. This field is the one causing electric currents within the superconductor borders, in the first few millimeters, as can be verified in Fig. 12.

For a magnetic field frequency of 5 Hz obtained from Eqs. (1) and (2), the power losses densities in the ZFC vehicle were estimated for different magnetic field amplitudes, as shown in Fig. 15. For 1 mT, the power loss density found was about $5,5 \times 10^{-5} \text{ W/cm}^3$. As the losses are proportional to the frequency of the magnetic field, these can be plotted as function of the ZFC-Maglev speed, as shown in Fig. 16.

Fig. 12, shows that the electric currents are condensed near the surfaces of the superconductors. Thus, the volume considered to calculate the YBCO power losses was restricted to a 1 mm shell near the superconductor surface. Knowing the total power losses, it was then possible to estimate the consumption of liquid nitrogen in a cryostat to be used in the ZFC-Maglev. Since the cryostat has a pressure valve, the heating process of the cooled superconductors was assumed produced at constant pressure, allowing use of the Heat Law equation (11)

$$Q = mC_p\Delta T. \quad (11)$$

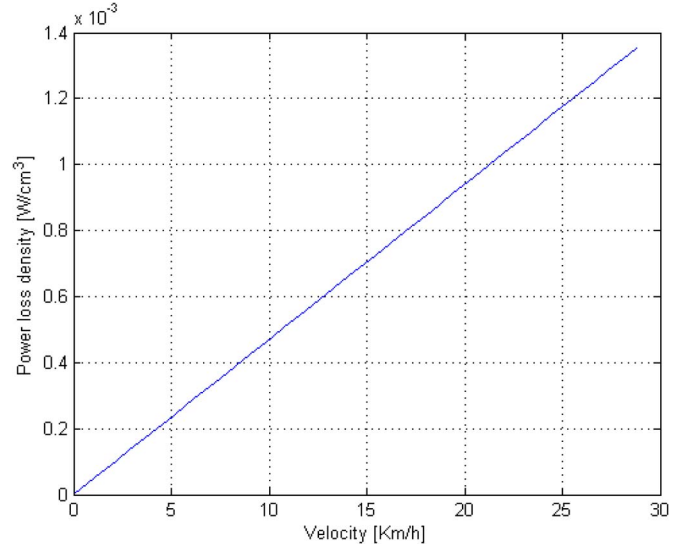


Fig. 16. Power loss density in function of the ZFC-Maglev speed.

In (11), the term m is the mass of liquid nitrogen (whose mass density is of 800 kg/m^3 and C_p its specific heat at constant pressure ($2,042 \times 10^3 \text{ Jkg}^{-1}\text{K}^{-1}$). The liquid nitrogen is at a temperature of 77 K, and evaporates at a temperature of 78 K. Thus, it was possible estimate the consumption of the deposit using (11) for $\Delta T = 1$ and $Q = P_{\text{loss}}t$

$$t = \frac{mC_p}{P_{\text{loss}}}. \quad (12)$$

To analyze the efficiency of the ZFC-Maglev in terms of liquid nitrogen consumption, the volume of liquid nitrogen was calculated for a possible time operation around 12 hours a day. Using the results plotted in Fig. 15 and also the simplified thermal model (12) for a field frequency of 5 Hz, the power loss density was estimated to be about $5,5 \times 10^{-5} \text{ W/cm}^3$. As the power losses are proportional to the frequency, the losses can be computed for other frequencies proportionally or, in other words, for different vehicle speeds, as shown in Fig. 16.

VII. CONCLUSION

The results achieved show that the Joule losses in the superconductors of the ZFC-Maglev are more significant for higher speeds of the vehicle. In this condition, the Joule losses and the aerodynamic losses move apart. This means that the total vehicle losses will be mainly caused by the aerodynamic effect for lower speeds. For higher speeds, the effect of the Joule losses in the superconductors will be high significant. This will occur because, in this situation, the variation of the magnetic field is higher, inducing larger electric currents in the superconductors. PMs with the best homogeneity have a variation in the amplitude of minimum 1%. This inhomogeneity transferred into the PM rail here. In the consequence, although small, the rail magnetic inhomogeneity causes decay in the pendulum—like vehicle movement. The loss is hysteretic and it goes nonlinear with the vehicle speed (namely $P \sim \Delta B^3$).

Further studies need to be done concerning now the “traditional” FC-Maglev, comparison with the ZFC-Maglev in terms of losses in the superconductors and associated operational costs.

To a rational comparison with a FC Maglev type, the Maglev-Cobra [4], [5] will be used by our group as an example of the FC topology. For this, the ZFC-Maglev has to be scaled-up to fulfill the set of specifications and functional criteria (levitation and guidance forces) equal to those of the Maglev-Cobra.

The results achieved will have to be analyzed and compared with those obtained from direct measurement of the Maglev-Cobra, allowing a characterization of the energetic consumption and the operational costs associated between the type-ZFC superconductor vehicle and the Maglev-Cobra superconductor vehicle.

Although not identical to the movement on the rail, the pendulum set up contains low curvature points, which include low significant centripetal acceleration. Also, concerning any movement characteristic of liquid nitrogen, the vehicle experiments either on the rail or in the pendulum setup were all effectuated

only when the LN₂ has been evaporated from the vessel were they are inserted. Concerning any LN₂ mass dependence, the same comment is applied as before. Hence, it is our assumption that those conditions will not affect the uncertainty of results more than 10% of magnitude.

REFERENCES

- [1] B. Painho, J. A. Dente, and P. J. Costa Branco, “Superconductor losses and damping effects under zero field cooling and field cooling conditions in a HTSC-magnet levitation system,” *J. Supercond. Novel Magn.*, vol. 24, no. 1/2, pp. 927–937, 2011.
- [2] P. J. Costa Branco and J. A. Dente, “Design and experiment of a new Maglev design using zero field-cooled YBCO superconductors,” *IEEE Trans. Ind. Electron.*, vol. 59, no. 11, pp. 4120–4127, Nov. 2012.
- [3] H. Jing *et al.*, “A high-superconducting Maglev system using T-shaped permanent magnet single-guideway,” *IEEE Trans. Appl. Supercond.*, vol. 18, no. 2, pp. 795–798, Jun. 2008.
- [4] G. G. Sotelo *et al.*, “Tests with one module of the Brazilian Maglev-Cobra vehicle,” *IEEE Trans. Appl. Supercond.*, vol. 23, no. 3, Jun. 2013, Art. ID 3601204.
- [5] G. G. Sotelo *et al.*, “A full scale superconducting magnetic levitation (MagLev) vehicle operational line,” *IEEE Trans. Appl. Supercond.*, vol. 25, no. 3, Jun. 2015, Art. ID 3601005.